

Supporting Information for

Tunneling and barrier-less motions in the 2- fluoroethanol···water complex: a rotational spectroscopic and ab initio study

*Wenyuan Huang, Javix Thomas, Wolfgang Jäger, and Yunjie Xu**

Department of Chemistry, University of Alberta, Edmonton, Alberta T6G 2G2, Canada

*E-mail: yunjie.xu@ualberta.ca. Fax: 1-780-492-8231.

Contents

Table S1 Calculated energies and spectroscopic constants of the 2-FE monohydrate.	S2
Figure S1 Relative energies of I , II , and the transition state of OH wagging.	S2
Figure S2 QTAIM and NCI plots of 2-FE and 2-FE···FE	S3
Table S2 Measured transition frequencies of 2-FE	S3
Table S3 Measured transition frequencies of the D isotopologues of 2-FE	S4
Completion of Ref. 30.	S5

Table S1. ZPE corrected (ΔE_0) and ZPE/BSSE corrected (ΔE_0^{BSSE}) energies (in kJ mol^{-1}), rotational constants (in MHz), and electric dipole moments (in Debye) of the three most stable conformers of 2- $\text{FE}\cdots\text{water}$ at the B3LYP-D3BJ/6-311++G(2d,p) level of theory.

Parameters	iG+g- I	iG+g- II	aG+g- III	aG+g- IV	aG+g- V	iG+t VI
ΔE_0^{a}	0.00	0.79	5.35	8.46	13.11	14.22
$\Delta E_0^{\text{BSSE b}}$	0.00	0.81	4.30	7.14	11.49	14.12
A	4898	4869	6093	13953	5995	4759
B	3464	3469	2401	1526	2386	3300
C	2193	2179	2082	1458	2056	2163
$ \mu_a $	0.61	0.88	0.00	1.33	1.20	4.85
$ \mu_b $	1.52	1.53	1.19	0.54	1.01	1.01
$ \mu_c $	0.31	2.03	0.56	1.38	0.20	0.41

^a Zero-point-energy corrected electronic energy relative to the lowest energy conformer, iG+g- I.

^b Zero-point-energy and counterpoise-corrected energy relative to iG+g- I.

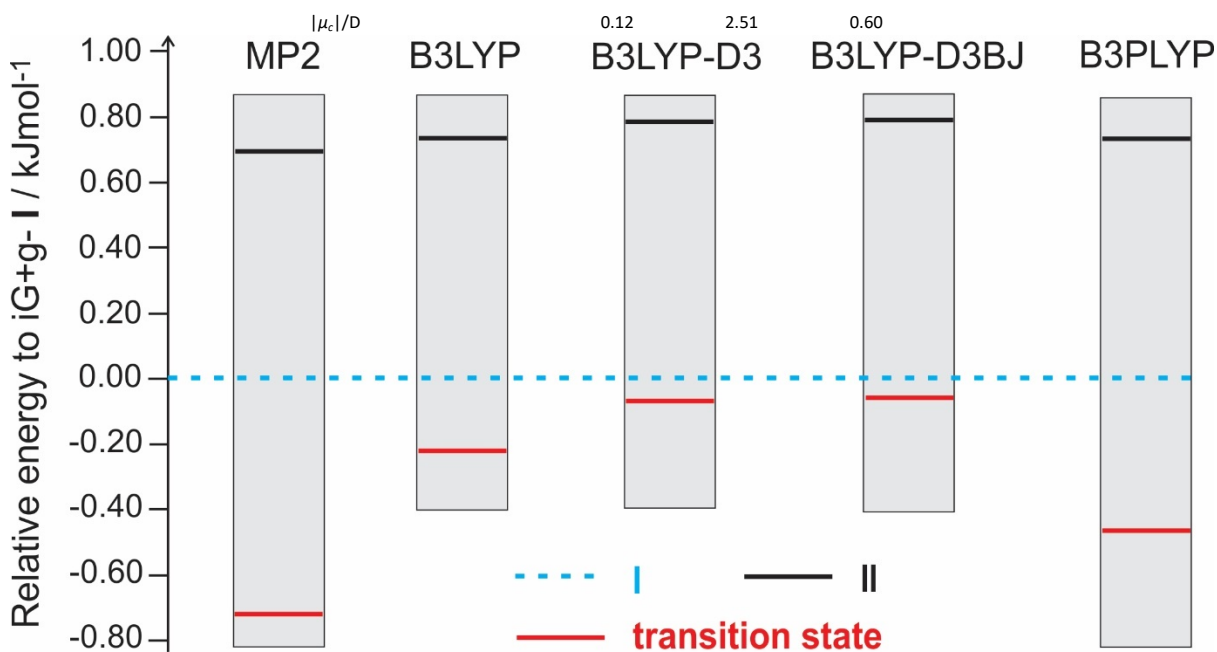


Figure S1. The relative energy values for iG+g- I, iG+g- II, and the transition state for the wagging motion with zero point energy correction at different levels of theory. All the relative values are with respect to iG+g- I. Please note that iG+g- II is predicted to be less stable than iG+g- I in all cases, while the transition state is predicted to be lower in energy than iG+g- I after zero-point-energy correction, indicating that the wagging motion is barrier-less.

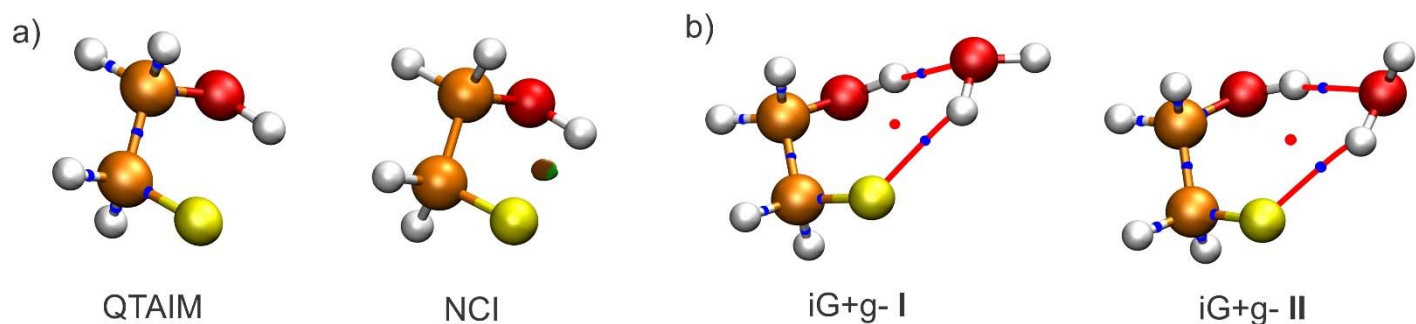


Figure S2. a) QTAIM and NCI plots of the 2-FE monomer. The attractive interaction between OwH...F contact is indicated by the small green surface. The brown surface represents the repulsive interaction mainly between the F and O atoms. b) QTAIM plots of the two most stable minima of 2-FE...H₂O.

Table S2. Measured rotational transition frequencies of the para and ortho states of the most stable 2-FE...H₂O conformer.

J'	Ka'	Kc'	J''	Ka''	Kc''	Para		Ortho	
						$\nu_{\text{exp}}/\text{MHz}$	$\Delta\nu^{\text{a}}/\text{kHz}$	$\nu_{\text{exp}}/\text{MHz}$	$\Delta\nu^{\text{a}}/\text{kHz}$
1	1	1	0	0	0	7125.4017	-4.9	7125.4245	-1.3
2	0	2	1	1	0	7828.3701	-0.8	7828.3518	-0.6
1	1	0	0	0	0	8319.2198	2.7	8319.2809	-2.0
2	2	1	2	1	2	8345.4033	-0.4	8345.4679	3.0
2	2	0	2	1	2	8809.8846	1.3	8809.9701	0.7
2	0	2	1	1	1	9022.1854	4.0	9022.2066	-2.9
3	3	1	3	2	1	9183.3204	-0.4	9183.3345	2.7
2	1	2	1	1	1	9880.9145	-1.2	9880.9326	4.3
3	2	2	2	1	2			10386.8100	-4.3
2	0	2	1	0	1	10610.1973	5.6	10610.1973	-7.1
3	0	3	2	1	1	10644.3243	-3.2		
3	3	1	3	2	2	11175.0730	1.6	11175.1035	-3.6
4	1	3	4	0	4	11273.2887	0.1	11272.9882	-0.5
3	3	0	3	2	2	11298.7104	-1.5	11298.7544	1.5
2	1	2	1	0	1	11468.9262	0.3	11468.9262	3.0
2	1	1	1	1	0	12268.4737	-2.2	12268.5307	2.8
3	1	2	2	2	1	13263.9648	0.1	13263.9110	5.2
3	0	3	2	1	2	14225.6980	-0.2	14225.6875	-4.7
3	1	3	2	1	2	14570.4460	-3.9	14570.4460	-0.8
2	1	1	1	0	1	15050.2917	-5.0		
3	0	3	2	0	2	15084.4356	3.2	15084.4105	-0.5
3	1	3	2	0	2	15429.1877	3.5	15429.1657	0.1
2	2	1	1	1	0			17032.5391	3.1
2	2	0	1	1	0	17496.9895	1.0		

^a $\Delta\nu = \nu_{\text{exp}} - \nu_{\text{cal}}$.

Table S3. Measured rotational transition frequencies of the seven D substituted most stable 2-FE \cdots H₂O conformer.

J'Ka'Kc'- J''Ka''Kc''	2FE \cdots DOH		2FE \cdots HOD		2FE \cdots D ₂ O		2FEOD \cdots DOH	
	ν_{exp} /MHz	$\Delta\nu^a$ /kHz	ν_{exp} /MHz	$\Delta\nu^a$ /kHz	ν_{exp} /MHz	$\Delta\nu^a$ /kHz	ν_{exp} /MHz	$\Delta\nu^a$ /kHz
111-000	7055.3598	1.4	7037.3551	-1.1	6972.7026	-0.6	6971.2649	0.3
221-212	8226.2280	-5.7	8119.0322	-5.6	8035.6160	-8.9	8149.0485	-0.4
110-000	8305.0481	1.4	8562.5364	1.4	8519.4537	4.3	8150.2602	-7.4
202-111	8870.1313	6.4	8392.1257	2.9	8261.0474	-0.9	8861.7857	-1.3
212-111	9744.7883	-0.5	9447.9188	1.1	9328.5932	-3.0	9686.6741	-4.0
322-313	10303.5597	1.7						
202-101	10467.6143	-4.9	10164.6452	1.1	10037.9691	2.0	10400.7794	-1.3
212-101	11342.2836	0.5	11220.4412	2.2	11105.5254	10.4	11225.6645	-7.3
211-110	12086.4905	7.2	11611.1944	-7.3	11454.3908	1.4	12042.1889	6.9
303-212	14017.7270	-14.0	13488.5233	-7.6	13304.3175	-4.2	13952.5235	-5.2
313-212	14374.7554	4.8	13971.8533	1.9	13798.8935	6.1	14279.8308	3.4
211-101	14854.8522	-0.7	14465.4135	9.0	14294.2352	5.3	14758.9599	-0.1
303-202	14892.4019	-3.0	14544.3320	6.2	14371.8628	-6.8	14777.4126	-7.2
313-202	15249.4258	11.3	15027.6445	-1.8	14866.4382	3.0	15104.7274	8.9
221-110	16878.9558	-4.5	16928.7675	-3.6	16785.1163	-7.6	16659.1686	7.2

J'Ka'Kc'- J''Ka''Kc''	2FEOD \cdots HOD		2FEOD \cdots H ₂ O		2FEOD \cdots D ₂ O	
	ν_{exp} /MHz	$\Delta\nu^a$ /kHz	ν_{exp} /MHz	$\Delta\nu^a$ /kHz	ν_{exp} /MHz	$\Delta\nu^a$ /kHz
111-000	6956.8538	2.5	7044.2245	-7.9	6889.9123	6.9
221-212	8410.4200	1.0	8243.2325	4.4	7960.5269	-7.0
110-000			8201.4031	-8.6	8358.6991	-5.1
202-111	8390.2066	0.6	9005.4451	-5.1	8265.9040	-2.0
212-111	9394.7509	-7.5	9819.6941	6.8	9277.8685	-6.0
202-101	10105.5903	-3.7	10540.2880	-6.4	9981.5278	-2.3
212-101	11110.1575	11.1	11354.5258	-5.8	10993.4984	-0.2
211-110	11570.9226	1.3	12217.5591	2.4	11419.0947	2.5
303-212	13436.7484	4.1	14153.0429	-4.4	13258.9776	-4.7
313-212	13885.9246	-2.4	14471.7669	0.0	13716.0138	8.1
211-101	14374.4147	1.7	14951.3988	2.3	14205.3516	6.8
303-202	14441.2924	-4.2	14967.2863	1.9	14270.9436	-7.2
313-202	14890.4824	3.0	15286.0060	1.9	14727.9781	3.9
221-110	16717.0682	-5.4	16822.1120	8.6	16565.9513	1.2

$$^a\Delta\nu = \nu_{\text{exp}} - \nu_{\text{cal}}$$

Table S4. Comparison of the substitution and theoretical coordinates.

	Exp.	iG+g- I		iG+g- II		Exp.	iG+g- I		iG+g- II		Exp.	iG+g- I		iG+g- II	
H9						H11					H12				
a	± 0.823	0.835	0.810	a	± 1.496	1.637	1.673	a	± 2.997	3.001	2.865				
b	± 1.100	1.129	1.129	b	± 0.922	-0.906	-0.888	b	± 0.000	-0.291	-0.193				
c	± 0.213	-0.292	-0.220	c	± 0.248	0.009	0.073	c	± 0.429	-0.351	0.760				

Completion of Ref. 30.

Gaussian 09 (Revision D.01), M. J. Frisch, G. W. Trucks, H. B. Schlegel, G. E. Scuseria, M. A. Robb, J. R. Cheeseman, G. Scalmani, V. Barone, B. Mennucci, G. A. Petersson, H. Nakatsuji, M. Caricato, X. Li, H. P. Hratchian, A. F. Izmaylov, J. Bloino, G. Zheng, J. L. Sonnenberg, M. Hada, M. Ehara, K. Toyota, R. Fukuda, J. Hasegawa, M. Ishida, T. Nakajima, Y. Honda, O. Kitao, H. Nakai, T. Vreven, J. A. Montgomery, Jr., J. E. Peralta, F. Ogliaro, M. Bearpark, J. J. Heyd, E. Brothers, K. N. Kudin, V. N. Staroverov, T. Keith, R. Kobayashi, J. Normand, K. Raghavachari, A. Rendell, J. C. Burant, S. S. Iyengar, J. Tomasi, M. Cossi, N. Rega, J. M. Millam, M. Klene, J. E. Knox, J. B. Cross, V. Bakken, C. Adamo, J. Jaramillo, R. Gomperts, R. E. Stratmann, O. Yazyev, A. J. Austin, R. Cammi, C. Pomelli, J. W. Ochterski, R. L. Martin, K. Morokuma, V. G. Zakrzewski, G. A. Voth, P. Salvador, J. J. Dannenberg, S. Dapprich, A. D. Daniels, O. Farkas, J. B. Foresman, J. V. Ortiz, J. Cioslowski, D. J. Fox, Gaussian, Inc., Wallingford CT, **2013**.